

Improved Access to Linear Tetrameric Hydroxamic Acids with Potential as Radiochemical Ligands for Zirconium(IV)-89 PET Imaging

Christopher J. M. Brown,^A Michael P. Gotsbacher,^{id A} and Rachel Codd^{id A,B}

^ASchool of Medical Sciences, The University of Sydney, Sydney, NSW 2006, Australia.

^BCorresponding author. Email: rachel.codd@sydney.edu.au

Two new linear tetrameric hydroxamic acid ligands (**3** and **4**) have been prepared as potential radioligands for immunological Zr^{IV}-89 positron emission tomography (PET) imaging. The ligands were prepared by conjugating *endo*-hydroxamic acid amino carboxylic acid (*endo*-HXA) monomers 5-[(5-aminopentyl)(hydroxy)amino]-5-oxopentanoic acid (PPH) or 2-(2-((2-(2-aminoethoxy)ethyl)(hydroxy)amino)-2-oxoethoxy)acetic acid (PPH^{NO}C^O) to trimeric desferrioxamine B (DFOB). The properties of DFOB-PPH (**3**) and DFOB-PPH^{NO}C^O (**4**) were compared with the first-in-class ligand DFO* (named DFOB-PBH (**2**) in the present work) and DFOB (**1**). In the initial phase of an Fe^{III}:Zr^{IV} competition experiment, **1** preferentially formed Fe^{III}-**1**, with Zr^{IV}-**1** becoming dominant after 48 h. Tetrameric **2–4** selected Zr^{IV} above Fe^{III} at all times. The initial rates of formation of Zr^{IV}-**3** and Zr^{IV}-**4** were greater than Zr^{IV}-**2**, which could reflect a better match between the Zr^{IV} ionic radius and the increased volume of the coordination sphere provided by **3** and **4**. In the presence of excess EDTA, Zr^{IV}-**4** dissociated more rapidly than Zr^{IV}-**2** and Zr^{IV}-**3**, which indicated that any beneficial increase in water solubility conferred by the presence of ether oxygen atoms in **4** could be offset by a reduction in complex stability. Outer-sphere solvation of the ether oxygen atoms in Zr^{IV}-**4** may increase the entropic contribution to the dissociation of the complex. The rank order of the initial rate of Zr^{IV} complexation in the presence of equimolar Fe^{III} (highest to lowest) **4** > **3** > **2** >>> **1** together with the rate of the dissociation of the Zr^{IV} complex (lowest to highest) **2** ≈ **3** > **4** >>> **1** identifies **3** as a ligand with potential value for immunological Zr^{IV}-89 PET imaging.

Manuscript received: 15 October 2019.

Manuscript accepted: 2 December 2019.

Published online: 27 February 2020.

Introduction

The hydroxamic acid functional group provides a rich, interdisciplinary research platform in coordination chemistry, chemical biology, biotechnology, and drug discovery.^[1,2] Hydroxamic acids are present in a subset of bacterial siderophores as functional groups that complex Fe^{III} from the local surroundings with a subsequent cascade that ultimately delivers Fe^{III/II} to the source cell for growth. The fundamental roles played by siderophores in nature and their potential applications in metal sequestration in the realms of health and the environment have inspired a large body of research.^[3–9] One application of siderophores is as multidentate ligands for the coordination of radiometals for use in nuclear medicine.^[10–13] The utility of hydroxamic acids to coordinate the radiometal zirconium(IV)-89 is the focus of the current work.

The archetypal hydroxamic acid siderophore desferrioxamine B (DFOB, **1**)^[14] has been used to coordinate Zr^{IV}-89 in multiple studies focussed on immunological positron emission tomography (PET) imaging.^[15–18] The terminal amine group of DFOB is not involved in the coordination sphere and provides a conjugation point for biomolecules, including antibodies, for immunological applications. The utility of Zr-89 arises from its 3.3-day half-life, which is complimentary to the circulation half-life of

antibodies. This allows a Zr-89-antibody complex to accumulate at the antigen-displaying tumour to enhance image resolution. The low positron emission energy of Zr-89 ($\beta^+ = 22.3\%$, $E_{av}(\beta^+) = 0.397$ MeV, $R_{av}(\beta^+) = 1.18$ mm) allows spatial resolution similar to F-18 ($R_{av}(\beta^+) = 0.69$ mm).^[19] Multiple pre-clinical and clinical studies have shown the promise of immunological Zr-89 PET imaging.^[20–23] Trimeric DFOB does not saturate the higher-coordination-number preference of Zr^{IV},^[24,25] which can increase the lability of Zr^{IV}-DFOB complexes, with animal studies indicating the deposition of leached Zr-89 in bone.^[26]

A more stable complex with Zr^{IV} was formed with a tetrameric analogue of DFOB prepared from the chain-extension reaction between DFOB and the *endo*-hydroxamic acid amino carboxylic acid (*endo*-HXA) monomer 4-((5-aminopentyl)(hydroxy)amino)-4-oxobutanoic acid (PBH).^[27] Other work has produced tetrameric macrocyclic hydroxamic acids using Zr^{IV} as a template to select its optimal *endo*-HXA monomer for the assembly of a 1 : 4 Zr^{IV} : ligand pre-complex before in situ ring closure.^[28] This metal-templated synthesis (MTS) approach showed Zr^{IV} selected the *endo*-HXA 5-[(5-aminopentyl)(hydroxy)amino]-5-oxopentanoic acid (PPH) in higher concentrations above PBH for macrocycle assembly,

with both the PPH- and PBH-based macrocycles forming Zr^{IV} complexes more stable than linear counterparts.^[28] The chain-extended DFOB tetramer, first named DFO*,^[27] and referred to in other work as DFOB-PBH (**2**), had limited water solubility, which prompted the generation of new tetrameric analogues that replaced four methylene groups in the backbone with four ether oxygen atoms. The ether-containing compound DFOB-O₃-PBH-O₁ was first produced using a combined microbiological-chemical approach,^[29] and later by total synthesis.^[30] Although the isosteric replacement of methylene groups with ether atoms successfully increased the water solubility of DFOB-O₃-PBH-O₁ above that of DFOB-PBH, access was limited by the microbiological-based production method. The multistep chemical synthesis of DFOB-O₃-PBH-O₁ may also be difficult to transition to a manufacturing setting.

The present work aimed to investigate a more efficient pathway to linear tetrameric hydroxamic acid ligands of the DFOB-PBH class using robust synthetic methods to broaden the range of ligands available for Zr-89 PET imaging. This notion directed the use of commercial and inexpensive DFOB as a synthon, as undertaken in the first work that adopted a chain-extension approach,^[27] and in a different ligand design.^[31] Recent work in the Codd group has improved the synthetic route towards *endo*-HXA monomers, and produced six new monomers containing variably positioned methylene, ether or thioether groups.^[32] The different properties of these *endo*-HXA monomers would confer different properties on the cognate DFOB-*endo*-HXA chain-extended construct. Here, we have prepared two new linear tetrameric hydroxamic acids with properties predicted to straddle the water solubility of DFOB-PBH. We describe the synthesis and characterisation of these compounds and aspects of Zr^{IV} coordination chemistry together with DFOB-PBH and DFOB.

Results and Discussion

Synthesis of Linear Tetrameric Hydroxamic Acids

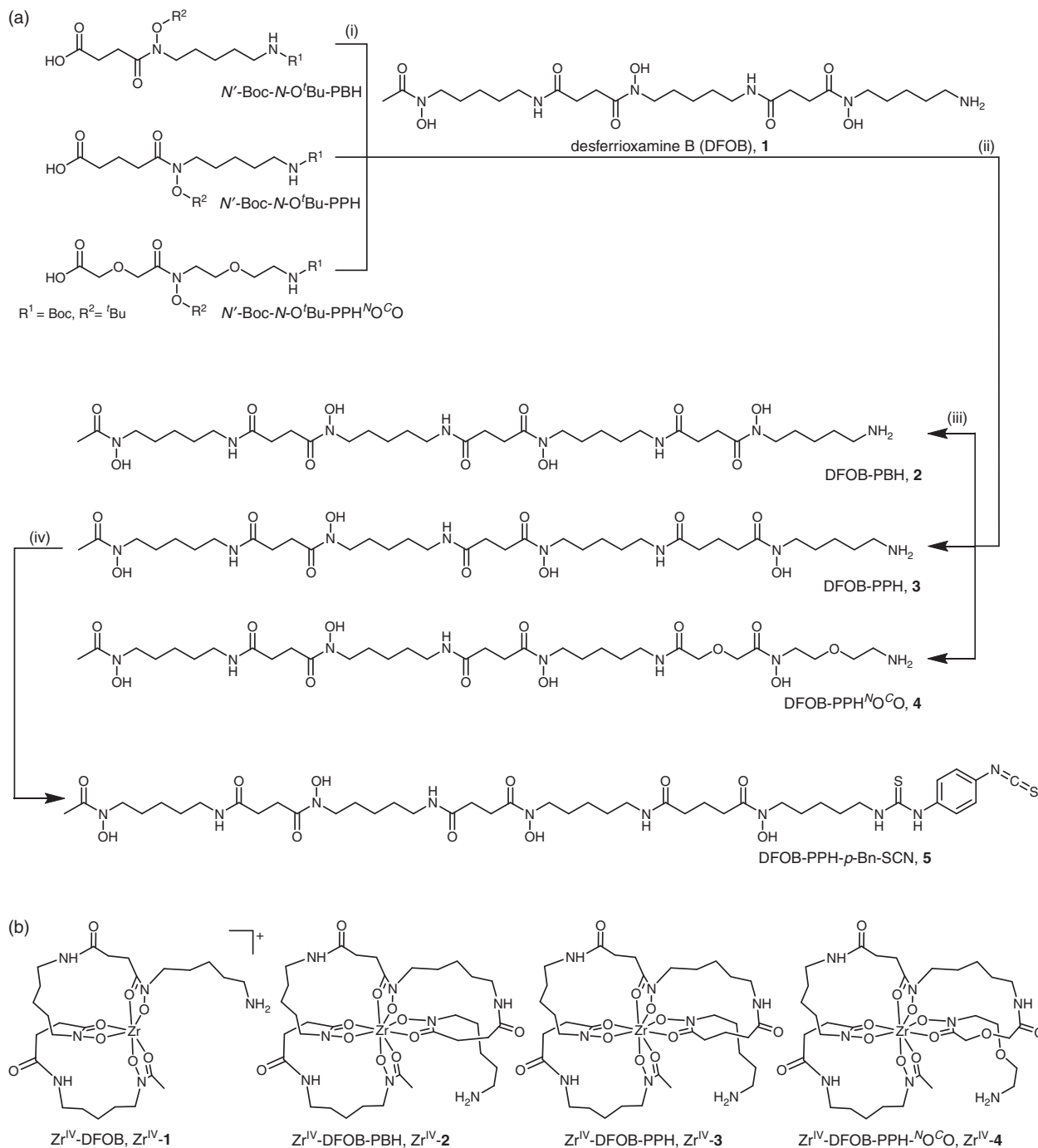
Two new linear tetrameric hydroxamic acids were prepared using a chain-extension reaction between DFOB and an *endo*-HXA monomer. The *endo*-HXA monomers were PPH or an analogue with two ether oxygen atoms positioned internal to the diamine- and dicarboxylic acid-containing region of the ligand, 2-(2-((2-(2-aminoethoxy)ethyl)(hydroxy)amino)-2-oxoethoxy)acetic acid (PPH^NO^CO). The synthesis of PPH and PPH^NO^CO has been described previously, with yields and synthetic efficiency improved above previous routes by the use of a 2-nitrophenylsulfonyl (nosyl) *N*-protecting group strategy.^[32] The *endo*-HXA monomer PBH was also prepared. Easier access to these *endo*-HXA monomers has expanded the types of tetramers able to be generated from conjugation reactions with DFOB. The chain-extension reaction was undertaken between the *N*-hydroxysuccinimide (NHS)-activated derivative of the *N*-Boc, *N*-O^tBu-protected *endo*-HXA, and DFOB, with global deprotection using 9 : 1 TFA/DCM. The *N*-O^tBu protecting group was selected to circumvent generating amide products from the over-reduction of *N*-OBn protecting groups, although the harsh conditions needed to be time-controlled to reduce product fragmentation. The crude compounds were obtained in ~45% yield, with overall yields of ~12% following purification to >95% purity using HPLC. The final series of compounds characterised in this work were trimeric DFOB (**1**), and tetrameric DFOB-PBH (**2**), DFOB-PPH (**3**), and DFOB-PPH^NO^CO (**4**) (Scheme 1a).

Characterisation and Properties of **1–4** and Zr^{IV} Complexes

The ligands **2–4** were characterised using ¹H and ¹³C NMR spectroscopy (Figs S1–S3, Supplementary Material) and liquid chromatography–mass spectrometry (LC-MS). The ¹H NMR spectrum of **3** showed two triplets ascribable to the methylene groups α to the carbonyl groups of the glutaric acid region and an upfield quintet attributable to the internal methylene group. The ¹H NMR spectrum of **4** showed downfield singlets attributable to the methylene groups α to the carbonyl groups of the 2,2'-oxydiacetic acid region and downfield signals for the methylene groups α to the oxygen atom of the oxybis(ethanamine) region. The LC-MS traces using total ion current (TIC) detection mode showed a high level of purity for **1–4** (Fig. 1) and showed the ligands each formed a 1 : 1 complex with Zr^{IV} under mild conditions (Fig. 2). The experimental isotope patterns for the single-charged and double-charged species of **1–4** correlated with calculated patterns. The corresponding Zr^{IV} complexes (Scheme 1b) gave isotope patterns that incorporated the pattern distinctive of natural Zr^{IV}: ⁹⁰Zr (51.45), ⁹¹Zr (11.22), ⁹²Zr (17.15), ⁹⁴Zr (17.38), ⁹⁶Zr (2.80), and matched calculated values. The formation of the Zr^{IV} complexes was quantitative, based on the absence of the signal for the free ligand in the TIC trace. Under common LC conditions, the retention times of signals attributable to Zr^{IV}-**1**, Zr^{IV}-**2**, Zr^{IV}-**3**, and Zr^{IV}-**4** were less (ranging 2–2.7 min) than the corresponding free ligands **1–4**, which suggests that radiolabelling would not adversely affect the water solubility of the metal–ligand complex. The log *D*₇ values of **1–4** were measured in octanol/water (pH 7) in triplicate using the shake-flask method (Table 1). The log *D*₇ value determined for **1** (log *D*₇ –2.45) was in reasonable agreement with previous work (log *D*₇ –2.22).^[29] The log *D*₇ values of **2–4** were more positive than **1**, as would be expected as a result of the increased number of methylene units in the chain-extended structures. The log *D*₇ value of **3** was marginally more positive than **2**, which correlated with the additional methylene unit. Compound **4** had the most negative log *D*₇ value of the tetramers **2–4**, which was consistent with the presence of two ether oxygen atoms. The increase in rank order starting from the most negative value for experimental log *D*₇ and calculated log *P* values of **4** < **2** < **3** was consistent using two different algorithms, although the ranked position of **1** was variable.

Selectivity of **1–4** Towards Complexing Fe^{III} or Zr^{IV}

Compared with tridentate **1**, octadentate **2–4** were predicted to have a higher preference for complexing Zr^{IV} than Fe^{III}. The selectivity of **1–4** towards complexing Fe^{III} or Zr^{IV} was assessed from LC-MS measurements from solutions of **1–4** in the presence of Fe^{III} and Zr^{IV} with each component present in a 1 : 1 : 1 ratio. The formation of 1 : 1 complexes between **1–4** and Zr^{IV} or Fe^{III} was monitored at time intervals to 72 h, with a duplicate experiment conducted for **1** to 120 h (Fig. 3). The octahedral coordination sphere of a 1 : 1 complex between Fe^{III} and **2–4** would be saturated by three hydroxamic acid groups, with the fourth hydroxamic acid group not involved in the primary coordination sphere (Scheme S1a, Supplementary Material). Complexes of 4 : 3 Fe^{III}/**2–4** stoichiometry involving the coordination of the fourth hydroxamic acid group of three unique ligands to a fourth Fe^{III} centre (Scheme S1b, Supplementary Material) were not observed under the acidic LC conditions. This is consistent with the acidic conditions of the LC system promoting the formation of 1 : 1 Fe^{III}–hydroxamic acid complexes, as observed for other hydroxamic acid systems capable



Scheme 1. (a) Synthesis of **1–4** (conditions: (i) NHS, EDC, DCM, room temperature (rt), 24 h; (ii) Et₃N, DMF, 70°C, 24 h; (iii) 9 : 1 TFA/DCM, rt, 24 h), or **5** (conditions: (iv) 1,4-phenylenediisothiocyanate, isopropanol/H₂O/CHCl₃, Et₃N, rt, 24 h); and (b) Zr^{IV} complexes formed with **1–4**.

of forming Fe^{III} complexes with non-equimolar stoichiometries. At neutral pH, complexes of 2 : 3 stoichiometry are predominant between Fe^{III} and tetradentate dihydroxamic acids, with 1 : 1 complexes observed at pH values < 5.^[33–36]

Hexadentate **1** has been evolved by Nature to form a stable, coordinatively saturated complex with Fe^{III} (log K 30.6).^[37–39] In the presence of competing Zr^{IV}, **1** preferentially complexed Fe^{III} (Fig. 3a) up to 48–68 h, but after this time and up to at least 120 h, the Zr^{IV}-**1** complex became dominant. Over the 120-h time course, the Fe^{III}-**1** and Zr^{IV}-**1** complexation behaviour followed a linear trend. The stability constant of Zr^{IV}-**1** has not been determined (**note added in proof**: during the period

that this work was being conducted and in review/production, two studies were published that report the experimental (log $\beta = 40$)^[40] and calculated (log $\beta = 41$)^[41] formation constant of Zr^{IV}-DFOB), although these data indicate that the complex is more thermodynamically stable than Fe^{III}-**1**. These data are consistent with recent work that showed **1** immobilised on a gold-mercaptopyronic acid surface-bound Fe^{III}, Hf^{IV} or Zr^{IV} with the rank in affinity (lowest to highest) Fe^{III} < Hf^{IV} < Zr^{IV}.^[42] The competition between octadentate **2–4** and complexation with Fe^{III} or Zr^{IV} was distinct from the **1** system (Fig. 3b–d). Each of **2–4** selected Zr^{IV} above Fe^{III} from the initial time point and up to the final time point of 72 h. This is in accord

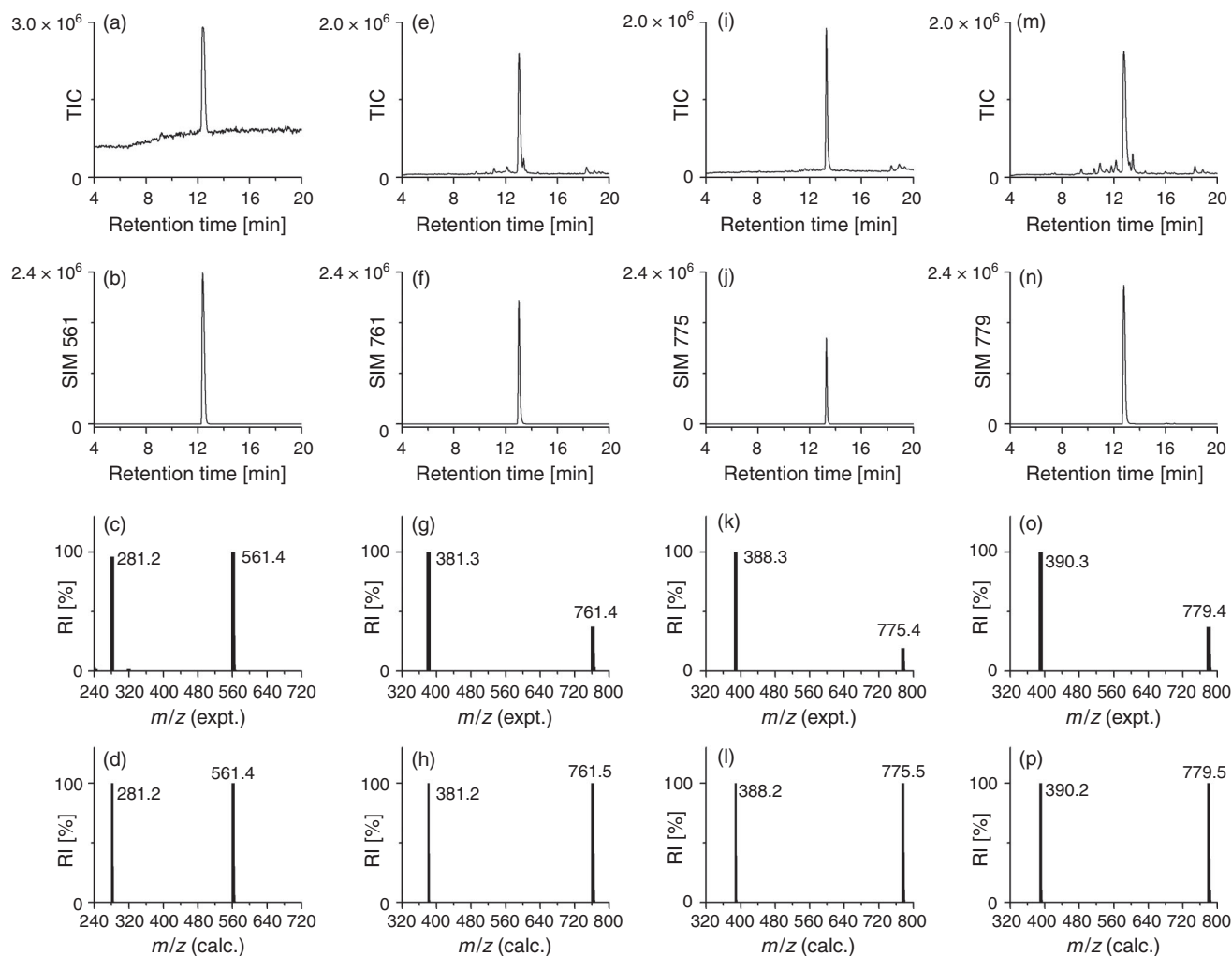


Fig. 1. LC-MS data from solutions of **1** (a–d), **2** (e–h), **3** (i–l), **4** (m–p), shown as total ion current (TIC) (first row), extracted ion chromatogram (second row), and experimental (third row) or calculated (fourth row) isotope patterns for the major single- or double-charged adducts. RI, relative intensity.

with the notion that the higher-dentate **2–4** ligands meet the higher coordination number preference of the Zr^{IV} coordination sphere to increase complex stability. There was a subtle difference in the profile between **2** (Fig. 3b) and the pair **3** and **4** (Fig. 3c–d). The complexation between Zr^{IV} and **2** showed a logarithmic trend, whereas that between Zr^{IV} and **3** or **4** showed asymptotic behaviour. The gradients of the linear regions ($r > 0.99$) of the fitted curves (Table 2) showed that the order from fastest to slowest with respect to the initial rate of Zr^{IV} complexation was $4 > 3 > 2 \gg \gg 1$.

Dissociation of Zr^{IV} -**1**, Zr^{IV} -**2**, Zr^{IV} -**3** or Zr^{IV} -**4** on Treatment with EDTA

The removal of Zr^{IV} from Zr^{IV} -**1**, Zr^{IV} -**2**, Zr^{III} -**3** or Zr^{IV} -**4** was examined by incubating the purified complex with a solution containing excess equivalents (160 or 1600) of EDTA at pH 7.4 to promote dissociation via trans-chelation. Aliquots were removed for analysis by LC-MS at time intervals to 3 days (Fig. 4). Data from the Zr^{IV} -**1** system were fitted at both EDTA concentrations with an asymptotic decay function, which reflected the rapid dissociation of hexadentate Zr^{IV} -**1** under these extreme in vitro conditions. The dissociation of Zr^{IV} complexes formed with octadentate ligands **2–4** was significantly attenuated compared with the hexadentate ligand **1**, as

consistent with the current understanding of Zr^{IV} coordination chemistry.^[10,15–19,24,25,27] Data from the Zr^{IV} -**2**, Zr^{III} -**3**, and Zr^{IV} -**4** systems were fitted at both EDTA concentrations with an exponential decay function with a linear fit to the initial dissociation (Table 2). For each of the Zr^{IV} -**2**, Zr^{III} -**3**, and Zr^{IV} -**4** systems, the rate of dissociation was greater with 1600 than with 160 excess equivalents of EDTA, which was unsurprising. The rate of dissociation was similar between Zr^{IV} -**2** and Zr^{IV} -**3** at both EDTA concentrations. Data for Zr^{IV} -**2**, Zr^{IV} -**3**, and Zr^{IV} -**4** at both EDTA concentrations suggested that Zr^{IV} -**4** dissociated more rapidly than Zr^{IV} -**2** and Zr^{IV} -**3**. Although Zr^{IV} -**4** appeared to form more rapidly than Zr^{IV} -**2** and Zr^{IV} -**3**, which could be useful for efficient radiolabelling, this potential advantage may be offset by a higher tendency for dissociation compared with the methylene-containing analogues.

The introduction of ether oxygen atoms into the main-chain region of **1** was first undertaken to improve the water solubility of downstream chain-extension reaction products, including DFOB- O_3 -PBH- O_1 .^[29] As weak donor atoms, the ether oxygen atoms were predicted not to impede hydroxamic acid-based coordination between Zr^{IV} and DFOB- O_3 -PBH- O_1 . In this work, compound **4** was produced as an easier-to-access ether-containing octadentate ligand for Zr^{IV} . The results from this work suggest that there may be potential liability in

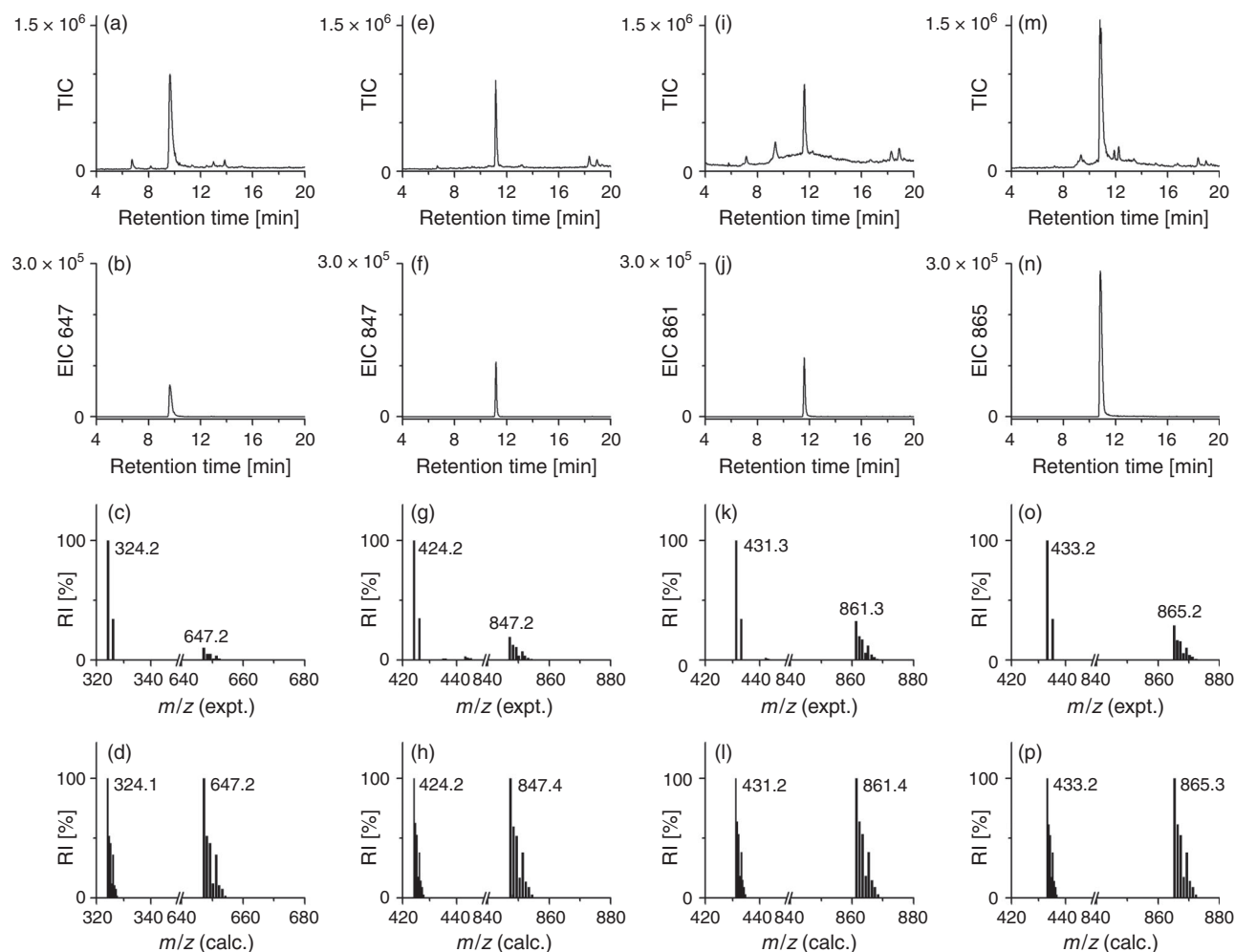


Fig. 2. LC-MS data from solutions of Zr^{IV} -1 (a–d), Zr^{IV} -2 (e–h), Zr^{IV} -3 (i–l), Zr^{IV} -4 (m–p), shown as total ion current (TIC) (first row), extracted ion chromatogram (second row), and experimental (third row) or calculated (fourth row) isotope patterns for the major single- or double-charged adducts.

Table 1. LC-MS parameters and experimental $\log D_7$ or calculated $\log P$ values for 1–4 and 1 : 1 Zr^{IV} complexes
ND, not determined; t_R , retention time

Name	Number	m/z $[M + H]^+$		t_R^A [min]	$\log D_7$		$\log P$	
		Obs	Calc		Obs ^B	Calc ^C	Calc ^D	
DFOB	1	561.4	561.4	12.37	−2.45 (±0.50)	−3.44	−2.75	
Zr^{IV} -DFOB	Zr^{IV} -1	647.2	647.2	9.64	ND	ND	ND	
DFOB-PBH	2	761.4	761.5	13.02	−1.70 (±0.12)	−3.71	−3.77	
Zr^{IV} -DFOB-PBH	Zr^{IV} -2	847.2	847.4	11.17	ND	ND	ND	
DFOB-PPH	3	775.4	775.5	13.28	−1.65 (±0.36)	−3.21	−3.55	
Zr^{IV} -DFOB-PPH	Zr^{IV} -3	861.3	861.4	11.60	ND	ND	ND	
DFOB-PPH ^N O ^C O	4	779.4	779.5	12.77	−2.07 (±0.41)	−4.85	−4.30	
Zr^{IV} -DFOB-PPH ^N O ^C O	Zr^{IV} -4	865.2	865.3	10.82	ND	ND	ND	

^AGradient of 0–100 % ACN/H₂O (40 min at 0.5 mL min^{−1}).

^BDetermined from shake-flask method (average of triplicate measurements, standard deviation in brackets).

^CDetermined as NH₃⁺ species using *Molinspiration* (<https://www.molinspiration.com/>).

^DDetermined as NH₃⁺ species using *ACD/Chemsketch*.

incorporating ether oxygen atoms into the design of octadentate hydroxamic acid ligands for Zr-89 PET imaging applications. It may be that the ether oxygen atoms promote solvation at the periphery and perhaps internally in the complex, with the propensity of the complex to dissociate increased by the entropic

contribution from the displacement of any ordered water molecules. This highlights the changes in properties that can occur with subtle structural modifications for this ligand class and supports ongoing studies of the properties of other analogues of DFOB produced using precursor-directed biosynthesis.^[43]

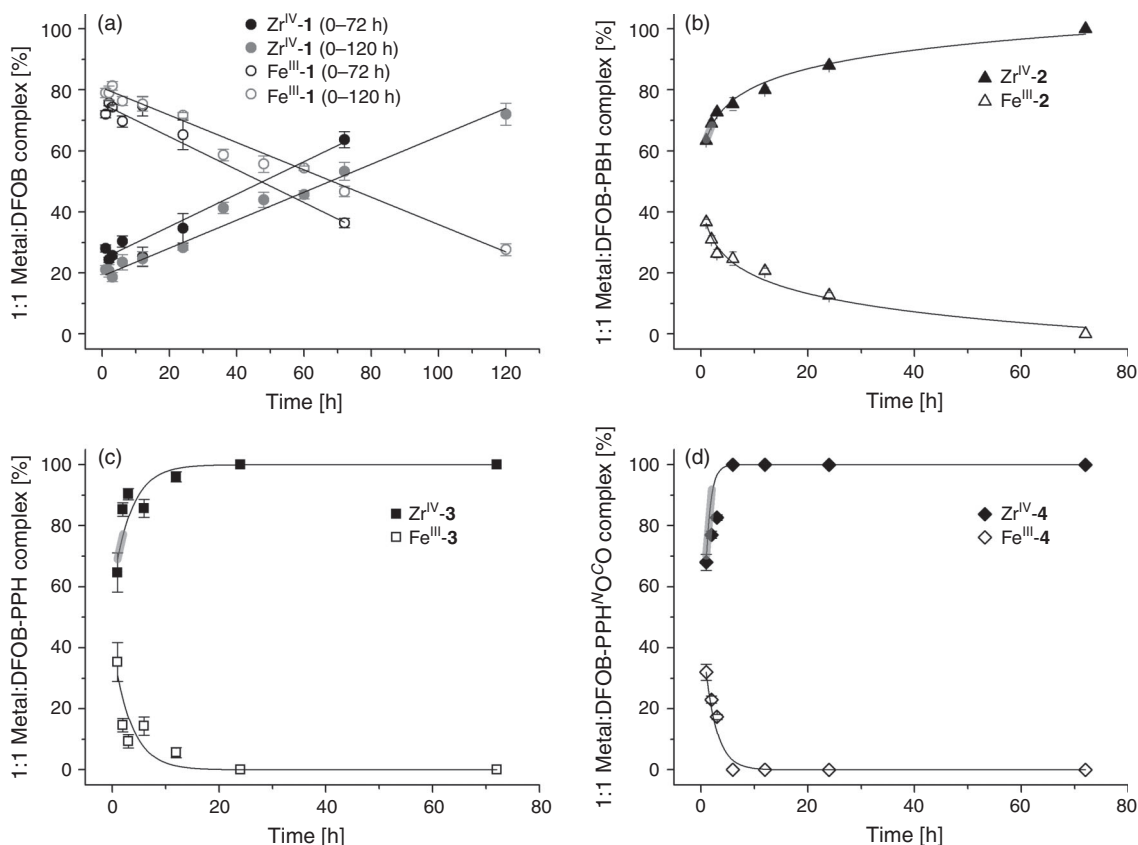


Fig. 3. Relative concentration of 1 : 1 complexes between Zr^{IV} or Fe^{III} and (a) 1, (b) 2, (c) 3, or (d) 4, formed from 1 : 1 : 1 solutions of $Zr^{IV}/Fe^{III}/1-4$, as a function of time. The region of linear fit is shown in grey.

Table 2. Gradients from the region of linear fit for the formation (load) of Zr^{IV-1} , Zr^{IV-2} , Zr^{IV-3} or Zr^{IV-4} , and the removal of Zr^{IV} (unload) via EDTA trans-chelation

Name	Number	Fit	Load	Gradient ^A	Fit	Unload	
						Gradient ^B Equivalents EDTA	
						1600	160
Zr^{IV} -DFOB	Zr^{IV-1}	Linear		0.53	Asymptotic	-497.4	-497.4
Zr^{IV} -DFOB-PBH	Zr^{IV-2}	Logarithmic		4.49	Exponential	-95.0 ^C	-47.6
Zr^{IV} -DFOB-PPH	Zr^{IV-3}	Asymptotic		7.72	Exponential	-97.2 ^D	-52.3 ^E
Zr^{IV} -DFOB-PPH ^{VO} C ^O	Zr^{IV-4}	Asymptotic		20.36	Exponential	-119.3 ^D	-83.6

^ATime interval: Zr^{IV-2} , Zr^{IV-3} , Zr^{IV-4} = 64 min.

^BTime interval: Zr^{IV-1} = 8.1 min; Zr^{IV-2} , Zr^{IV-3} , Zr^{IV-4} = 18 min.

^CData point at 3 d omitted to reduce the overparameterisation of the fitting function.

^DData point at 3 d omitted to maintain consistency within this system.

^EData point at 2 d omitted as an outlier.

This work suggests that the gain in water solubility that results from the isosteric replacement of methylene groups with ether atoms may be offset by a loss in complex stability, and that the preferred ligand type for Zr^{IV} complexation might exclusively contain methylene groups in the main-chain backbone. The first-in-class ligand of this type DFO*,^[27] which has been included in the present study as compound 2, meets this criterion. The current work indicates that analogue 3, which contains one additional methylene group in the dicarboxylic acid region, forms a complex with Zr^{IV} more rapidly than 2. Although at first pass it might be difficult to rationalise that the introduction of one methylene group in 3 could improve ligand

performance above 2, two supporting reasons are provided. First, the *endo*-HXA monomer PPH used in the chain-extension reaction to produce 3 was selected preferentially by Zr^{IV} above PBH (the *endo*-HXA used to produce 2) in the assembly of Zr^{IV} macrocycles using MTS.^[28] This suggests that PPH is preferred to PBH as a Zr^{IV} ligand. The volume of the coordination sphere of Zr^{IV-3} would be greater than Zr^{IV-2} and may be more suited to accommodating the Zr^{IV} ion. Second, other work has shown that the introduction of a single methylene group into a radiochemical ligand can significantly modulate properties and the stability of corresponding radiometal complexes.^[44]

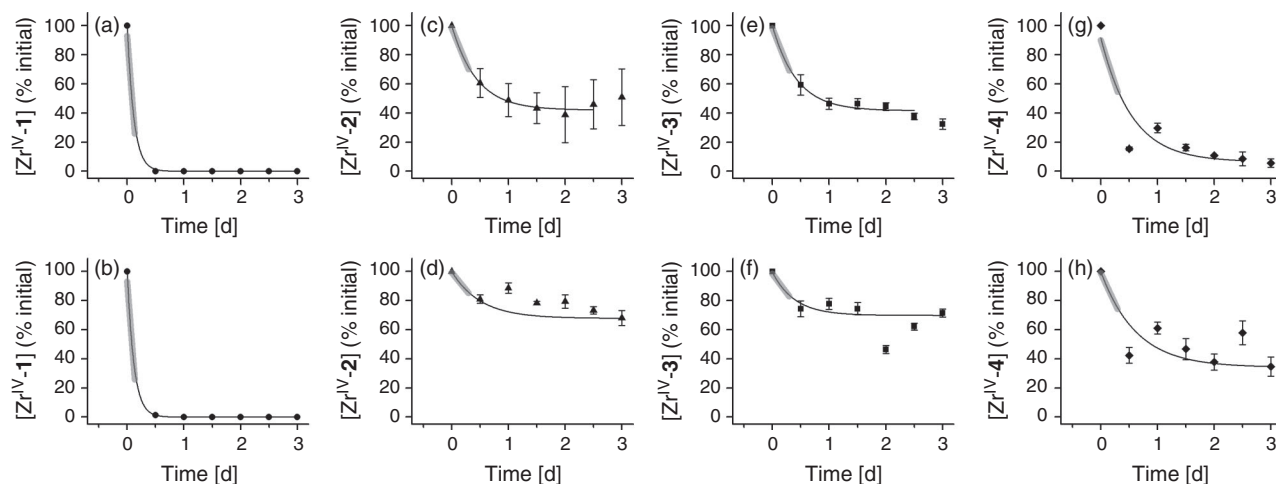


Fig. 4. Concentration (% of initial) of Zr^{IV}-1 (a, b), Zr^{IV}-2 (c, d), Zr^{IV}-3 (e, f), or Zr^{IV}-4 (g, h) as a function of time in the presence of EDTA (pH 7) at a 1600 (first row) or 160 (second row) excess of equivalents. The region of linear fit is shown in grey.

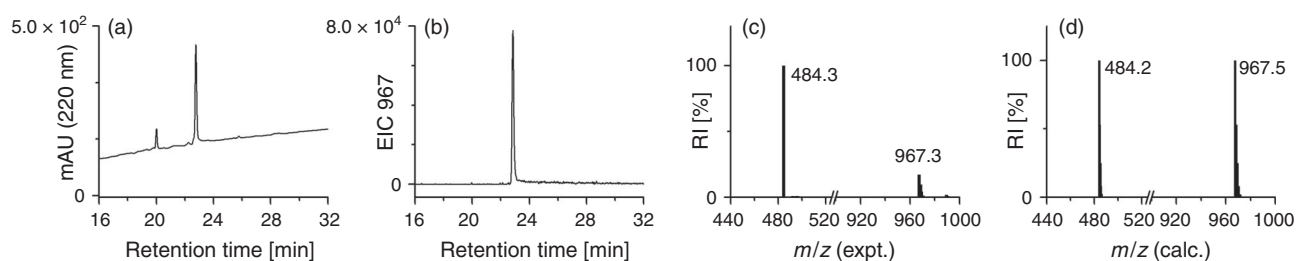


Fig. 5. LC-MS data from a solution of **5** using detection by (a) UV or (b) EIC, and (c) experimental or (d) calculated isotope patterns for the major single- or double-charged adducts.

Compound **3** was reacted with 1,4-phenylenediisothiocyanate (Scheme 1) to generate DFOB-PPH-*p*-Bn-SCN (**5**) for conjugation of amine-bearing biological vectors. Compound **5** was characterised using LC-MS (Fig. 5) and ¹H and ¹³C NMR spectroscopy (Fig. S4, Supplementary Material). Improved access to *endo*-HXA ligands including PPH will enable the synthesis of **3** and the activated product **5**, with the latter of potential use as a ligand for immunological Zr-89 PET imaging applications.

Conclusion

Two new linear tetrameric hydroxamic acid ligands, DFOB-PPH (**3**) and DFOB-PPH^NO^CO (**4**), were prepared from the corresponding *endo*-HXA monomers PPH and PPH^NO^CO. The properties of **3** and **4** were examined together with tetrameric DFOB-PBH (**2**) and trimeric DFOB (**1**). Compound **4** was designed as an easy-to-access water-soluble tetramer with high affinity for Zr^{IV}. Compound **4** was the most water soluble of **2**–**4**. The rank order of the initial rate of Zr^{IV} complexation (highest to lowest) of **1**–**4** in the presence of equimolar Fe^{III} was **4** > **3** > **2** >>> **1**. The favourable ranking of **4** in these measurements was offset by the rank order in the initial rate of dissociation of the Zr^{IV} complex (lowest to highest) in the presence of EDTA of **2** ≈ **3** > **4** >>> **1**. This identifies **3** as a linear tetrameric hydroxamic acid with potential in immunological Zr-89 PET imaging, with the activated compound DFOB-PPH-*p*-Bn-SCN (**5**) in hand for ongoing studies.

Experimental

All reactions were performed under an inert nitrogen atmosphere and reaction progress was monitored via LC-MS. ¹H and ¹³C

NMR spectroscopy were performed on a Bruker 600 MHz AVIII with TCI cryoprobe at 25°C operating with *Topspin 3.5* NMR software. Samples were made to a concentration of 5 mg mL⁻¹ in deuterated dimethyl sulfoxide ([D₆]DMSO, Sigma–Aldrich, 99.8%). Chemical shifts are reported in parts per million relative to the residual solvent peaks for DMSO (2.50 ppm (¹H), 39.52 ppm (¹³C)). Signal multiplicities are labelled as follows: s (singlet), d (doublet), t (triplet), q (quartet), qn (quintet), m (multiplet). Coupling constants (*J*) are reported in hertz.

Reagents

Desferrioxamine B mesylate (>92.5%), dichloromethane (≥99.8%), 1-ethyl-3-(3-dimethylaminopropyl)carbodiimide (EDC) (>99.0%), methanol (99.8%), *N,N*-dimethylformamide (99.8%), NHS (98%), 1-octanol (>99%), 1,4-phenylenediisothiocyanate (98%), triethylamine (>99.5%), trifluoroacetic acid (99%), zirconium(IV) acetylacetonate (97%), and iron(III) acetylacetonate (99.9%) were purchased from Sigma–Aldrich. Acetonitrile (HPLC grade) and chloroform were purchased from Thermo Fisher Scientific. All solvents were anhydrous unless stated otherwise. All chemicals were used as received. Milli-Q water was used for all experiments.

Instrumentation

Liquid Chromatography–Mass Spectrometry

Reverse-phase liquid chromatography–mass spectrometry (RP LC-MS) used an Agilent Technologies HPLC system consisting of an autoinjector (100 μL loop), an Agilent 1260 Infinity degasser, a quaternary pump, and an Agilent 6120 Series

Quadrupole electrospray ionisation (ESI) mass spectrometer. An Agilent C18 column RP prepacked column (4.6 × 150 mm ID, particle size 5 µm) was used for all experiments. Agilent *OpenLAB Chromatography Data System (CDS) ChemStation Edition* was used for data processing in the TIC or selected-ion monitoring (SIM) modes. All samples were made to a concentration of 1 mg mL⁻¹ in methanol. The following instrumental conditions were used: flow rate 0.5 mL min⁻¹, injection volume 5 µL, spray voltage 47 kV, capillary voltage 3 kV, capillary temperature 250°C, tube lens-offset 10 V. The mobile phase was prepared by mixing ACN/formic acid (99.9 : 0.1) and H₂O/formic acid (99.9 : 0.1). The method used a 0–100 % ACN/H₂O gradient over 45 min.

Semi-Preparative or Preparative HPLC

Semi-preparative or preparative HPLC was conducted on a Shimadzu LC-20 series LC system with two LC-20AP pumps, an SIL-10AP autosampler, a SPD-20A UV-vis detector, and a FRC-10A fraction collector. Shimadzu *LabSolutions* software (version 5.73) was used for data acquisition and processing. Shimadzu Shimpack GIS-C18 columns (preparative, 150 × 20 mm ID; semipreparative, 150 × 10 mm ID, particle size 5 µm) were used. The mobile phase consisted of ACN/TFA (99.95 : 0.05) and H₂O/TFA (99.95 : 0.05). Method (preparative): 2–25 % ACN/H₂O over 25 min at a flow rate of 20 mL min⁻¹. Method (semi-preparative): 40 : 60 ACN/H₂O from 0 to 10 min; 40 : 60 to 90 : 10 ACN/H₂O from 10 to 15 min; 90 : 10 ACN/H₂O from 15 to 25 min, with a flow rate of 5 mL min⁻¹.

Synthesis of DFOB-PBH (2), DFOB-PPH (3) or DFOB-PPH^NO^CO (4)

4-(*tert*-Butoxy(5-((*tert*-butoxycarbonyl)amino)pentyl)amino)-4-oxobutanoic acid (*N'*-Boc-*N*-O^tBu-PBH), 5-(*tert*-butoxy(5-((*tert*-butoxycarbonyl)amino)pentyl)amino)-5-oxopentanoic acid (*N'*-Boc-*N*-O^tBu-PPH) or 11-(*tert*-butoxy)-2,2-dimethyl-4,12-dioxo-3,8,14-trioxa-5,11-diazahexadecan-16-oic acid (*N'*-Boc-*N*-O^tBu-PPH^NO^CO) were prepared based on literature methods.^[32] To a solution of *N'*-Boc-*N*-O^tBu-PBH (370 mg, 0.99 mmol), *N'*-Boc-*N*-O^tBu-PPH (388 mg, 0.99 mmol) or *N'*-Boc-*N*-O^tBu-PPH^NO^CO (391 mg, 0.99 mmol) in DCM (20 mL) was added NHS (289 mg, 2.52 mmol), followed by the addition of EDC (390 mg, 2.52 mmol). The mixture was stirred at room temperature overnight. The mixture was washed once with water (20 mL) and the organic phase was collected. The aqueous phase was extracted with DCM (2 × 20 mL). The organic layers were combined, and the solvent was removed under vacuum to yield the NHS-activated monomer as an oil. A solution of the NHS-activated monomer, DFOB (415 mg, 0.74 mmol), and triethylamine (205 µL, 1.44 mmol) in DMF (10 mL) was stirred at 70°C overnight. The reaction was evaporated to dryness under vacuum and the resultant solid was washed with diethyl ether (5 × 5 mL) and water (5 × 5 mL). The compound was treated with a solution of TFA/DCM (9 : 1, 10 mL) at room temperature (rt) overnight. Analyses of the crude samples by LC-MS using UV detection showed the peak areas of the signals attributable to 2, 3 or 4 as 47, 43 or 41 % respectively of all species present. No starting material (1) was present. The mixture was concentrated under vacuum and purified via preparative HPLC to give DFOB-PBH (2), DFOB-PPH (3) or DFOB-PPH^NO^CO (4) with a purity of 95 % and an approximate overall yield of 12 %.

*N*1-(27-Amino-11,22-dihydroxy-7,10,18,21-tetraoxo-6,11,17,22-tetraazaheptacosyl)-*N*1-hydroxy-*N*4-(5-(*N*-hydroxyacetamido)pentyl)succinamide (DFOB-PBH) (2)

δ_H (600 MHz, [D6]DMSO) 9.64 (br s, 3H), 7.78–7.79 (m, 4H), 7.70 (s, 3H), 3.44–3.48 (m, 8H), 2.98–3.01 (m, 6H), 2.73–2.79 (m, 2H), 2.56–2.57 (m, 6H), 2.25–2.28 (m, 6H), 1.96 (s, 3H), 1.48–1.54 (m, 10H), 1.35–1.40 (m, 6H), 1.20–1.27 (m, 8H). δ_C (150 MHz, [D6]DMSO) 172.5, 172.4, 171.8, 170.6, 47.5, 47.3, 39.2, 38.9, 30.4, 30.3, 29.3, 28.0, 27.9, 27.1, 26.5, 26.2, 34.0, 24.0, 23.3, 20.8. *m/z* (LRMS ESI+) 381.3 ([M + 2H]²⁺, 100 %). These data are in agreement with the literature.^[27]

*N*1-(5-Aminopentyl)-*N*1-hydroxy-*N*5-(3,14,25-trihydroxy-2,10,13,21,24-pentaoxo-3,9,14,20,25-pentaazatriacontan-30-yl)glutaramide (DFOB-PPH) (3)

δ_H (600 MHz, [D6]DMSO) 9.59–9.66 (m, 4H, 4 × OH), 7.75–7.78 (m, 3H, 3 × NH), 7.65 (br s, 3H, NH₃·TFA), 3.43–3.49 (m, 8H, H-6, 18, 29, 40 (water peak underneath)), 2.98–3.01 (m, 6H, H-14, 25 36), 2.74–2.78 (m, 2H, H-2), 2.57 (t, *J* 7.0, 4H, H-21, 32), 2.33 (t, *J* 7.4, 2H, H-9), 2.26 (t, *J* 7.2, 4H, H-22, 33), 2.07 (t, *J* 7.4, 2H, H-11), 1.96 (s, 3H, H-43), 1.70 (qn, *J* 7.4, 2H, H-10), 1.48–1.56 (m, 10H, H-3, 5, 17, 28, 39), 1.37 (qn, *J* 7.4, 6H, H-15, 26, 37), 1.21–1.29 (m, 8H, H-4, 16, 27, 38). δ_C (150 MHz, [D6]DMSO) 172.9, 172.4, 172.1, 171.8, 170.6, 47.5, 47.2, 39.2 38.9, 38.8, 35.3, 31.7, 30.3, 29.3, 28.0, 27.1, 26.5, 26.2, 24.0, 23.4, 21.0, 20.8. *m/z* (LRMS ESI+) 388.3 ([M + 2H]²⁺, 100 %). *m/z* (HRMS) 775.49238; calc. for C₃₅H₆₇N₈O₁₁ ([M + H]⁺) 775.49243.

*N*1-(1-Amino-6,18-dihydroxy-7,11,19,22-tetraoxo-3,9-dioxa-6,12,18,23-tetrazaooctacosan-28-yl)-*N*1-hydroxy-*N*4-(5-(*N*-hydroxyacetamido)pentyl)succinamide (DFOB-PPH^NO^CO) (4)

δ_H (600 MHz, [D6]DMSO) 9.93 (s, 1H, OH), 9.64–9.68 (m, 3H, 3 × OH), 7.87–7.91 (m, 3H, NH₃·TFA), 7.79 (t, *J* 5.3, 3H, 3 × NH), 4.35 (s, 2H, H-11), 3.93 (s, 2H, H-9), 3.68 (t, *J* 5.6, 2H, H-6), 3.60 (q, *J* 5.3, 4H, H-3, 5), 3.45 (t, *J* 7.0, 6H, H-18, 29, 40 (water peak underneath)), 3.06–3.08 (m, 2H, H-14), 2.98–3.01 (m, 4H, H-25, 36), 2.95 (q, *J* 5.4, 2H, H-2), 2.57 (t, *J* 7.2, 4H, H-21, 32), 2.26 (t, *J* 7.3, 4H, H-22, 33), 1.96 (s, 3H, H-43) 1.48–1.50 (m, 6H, H-17, 28, 39), 1.35–1.44 (m, 6H, H-15, 26, 37), 1.21–1.23 (m, 6H, H-16, 27, 38). δ_C (150 MHz, [D6]DMSO) 172.4, 171.8, 169.3, 144.6, 143.9, 126.8, 71.0, 68.7, 66.7, 66.5, 47.5, 39.0, 38.9, 38.5, 30.4, 29.3, 28.1, 26.5, 24.0, 20.8. *m/z* (LRMS ESI+) 390.3 ([M + 2H]²⁺, 100 %). *m/z* (HRMS) 779.45109; calc. for C₃₃H₆₃N₈O₁₃ ([M + H]⁺) 779.45091.

Synthesis of DFOB-PPH-*p*-Bn-SCN (5)

DFOB-PPH (30 mg, 38 µmol) was dissolved in an isopropanol/water solution (3.8 mL/1 mL). A chloroform solution (4.8 mL) of 1,4-phenylenediisothiocyanate (75 mg, 390 µmol) was added, followed by the immediate addition of triethylamine (50 µL, 358 µmol) and the reaction was stirred overnight at room temperature. The reaction was concentrated by removing chloroform under vacuum. A white precipitate that formed in the remaining isopropanol solution was removed via centrifugation. The supernatant was purified by semipreparative HPLC and the sample was lyophilised to give a white powder. Yield 10 mg (27 %). δ_H (600 MHz, [D6]DMSO) 9.56–9.64 (m, 4H), 7.92 (br s, 1H), 7.73–7.78 (m, 4H), 7.54–7.55 (m, 2H), 7.36–7.37 (m, 2H), 3.44–3.49 (m, 10H), 2.98–3.01 (m, 6H), 2.57 (t, *J* 7.0, 4H), 2.33 (t, *J* 7.4, 2H), 2.26 (t, *J* 7.3, 4H), 2.07 (t, *J* 7.4), 1.96 (s, 3H)

1.69 (qn, J 7.5, 2H), 1.48–1.55 (m, 10H), 1.38 (qn, J 7.0, 6H), 1.17–1.27 (m, 8H). δ_C (150 MHz, [D6]DMSO) 172.4, 171.8, 126.7, 123.5, 47.5, 38.9, 38.8, 35.3, 31.7, 30.3, 29.3, 28.5, 28.0, 26.5. m/z (LRMS ESI+) 484.3 ($[M + H]^+$, 100%). m/z (HRMS) 967.47309; calc. for $C_{43}H_{71}N_{10}O_{13}S_2$ ($[M + H]^+$) 967.47397.

Formation of Zr^{IV} Complexes

$Zr^{IV}(\text{acac})_4$ (7 mg, 14.3 μmol) was dissolved in MeOH (10 mL) to give a 1.43 mM stock solution. An aliquot of the Zr^{IV} stock solution (1 mL) was added to DFOB (**1**) (1 mg, 1.78 μmol) or an aliquot (1.3 mL) added to DFOB-PBH (**2**) (1 mg, 1.31 μmol), DFOB-PPH (**3**) (1 mg, 1.29 μmol) or DFOB-PPH $^{NO^C}O$ (**4**) (1 mg, 1.28 μmol). The solutions were stirred at room temperature for 3 h and an aliquot (100 μL) was sampled for analysis using LC-MS.

EDTA Trans-Chelation Assay

DFOB (**1**), DFOB-PBH (**2**), DFOB-PPH (**3**) or DFOB-PPH $^{NO^C}O$ (**4**) (5 mg) was dissolved in MeOH (5 mL), $Zr^{IV}(\text{acac})_4$ (3 mg, 14.2 mmol) was added and the solution was stirred for 3 h. The solvent was removed under vacuum and the crude residue was dissolved in water (5 mL). The solution was loaded onto a Waters C-18 cartridge, which was washed with water (10 mL) to remove excess Zr^{IV} and with ACN/ H_2O (2 : 5) to collect Zr^{IV} -1, Zr^{IV} -2, Zr^{IV} -3 or Zr^{IV} -4. The ACN was removed under vacuum and the remaining aqueous solution was lyophilised. A stock solution (1 mg mL^{-1}) of Zr^{IV} -1, Zr^{IV} -2, Zr^{IV} -3 or Zr^{IV} -4 was prepared in MeOH. An aliquot of the stock solution (10 μL) was added to an aliquot (190 μL) of EDTA (10 mM or 100 mM) at pH 7.4. A reference sample for each of Zr^{IV} -1, Zr^{IV} -2, Zr^{IV} -3 or Zr^{IV} -4 was prepared by the addition of an aliquot of the stock solution (10 μL) to an aliquot (190 μL) of water. At each time point (0, 0.5, 1, 1.5, 2, 2.5, 3 days), 10 μL of the EDTA solution and 10 μL of the reference sample were removed for analysis by LC-MS using TIC as the detection mode. The EDTA solutions were analysed in triplicate (3 \times 10 μL aliquots at each time point) and the area under the curve (AUC) of signals for Zr^{IV} -1, Zr^{IV} -2, Zr^{IV} -3 or Zr^{IV} -4 were referenced against the AUC for the same species in the reference sample (single analysis). The stoichiometric excess of EDTA (from the 10 mM or 100 mM stock solutions) in the final solutions was as follows. Zr^{IV} -1: 123 or 1233; Zr^{IV} -2: 161 or 1612; Zr^{IV} -3: 164 or 1640; Zr^{IV} -4: 165 or 1645. The values 160 or 1600 were used as representative across the system.

Fe^{III} - Zr^{IV} Competition Assay

Samples of $Zr^{IV}(\text{acac})_4$ (3 mg, 6.2 μmol) and $Fe^{III}(\text{acac})_3$ (2.2 mg, 6.2 μmol) were prepared as a mixture in MeOH (5.2 mL). Samples of **1** (3.4 mg, 6.2 μmol), **2** (4.7 mg, 6.2 μmol), **3** (4.8 mg, 6.2 μmol), or **4** (4.8 mg, 6.2 μmol) were prepared in MeOH (5 mL). The solutions of **1–4** were added to the solution containing $Zr^{IV}(\text{acac})_4$ and $Fe^{III}(\text{acac})_3$ and the 1 : 1 : 1 $Zr^{IV}/Fe^{III}/\text{ligand}$ solution was incubated for 1 h. The pH of a representative solution was ~ 7.5 . An aliquot of the solution (200 μL) was removed and aliquots (10 μL) sampled at 1, 2, 3, 6, 12, 24, and 72 h for analysis by LC-MS using UV detection at 220 nm (with extinction coefficients equivalent between Zr^{IV} and Fe^{III} complexes), with AUC peak integration used to give the relative concentration of Zr^{IV} -1, Zr^{IV} -2, Zr^{IV} -3, Zr^{IV} -4, Fe^{III} -1, Fe^{III} -2, Fe^{III} -3, and Fe^{III} -4. The analysis was undertaken in triplicate (3 \times 200 μL subsampled). An additional experiment was conducted for **1** at 1, 2, 3, 6, 12, 24, 72 and 120 h.

Distribution Coefficients (Log D_7) Measurements

Distribution coefficients were determined by the shake-flask method using presaturated 1-octanol and MilliQ water. The pH of the water following equilibration was determined as pH 7.05. Presaturated 1-octanol (0.5 mL) was added to presaturated aqueous solutions of **1–4** (0.5 mL of 2 mg mL^{-1}) in an Eppendorf tube. Three solutions were set up for each of **1–4** (triplicate samples). The mixtures were shaken (250 rpm) on an orbital shaker for 20 h, aliquots of each phase (100 μL) were removed and added to MeOH (100 μL), and the solutions were analysed by LC-MS (detection mode: SIM) on a 0–30% ACN/ H_2O gradient over 40 min at a flow rate of 0.5 mL min^{-1} . The concentration of each compound was calculated for the aqueous and organic layers by integration of the peak area of the extracted ion chromatograms.

Supplementary Material

1D and 2D NMR spectroscopic data, HRMS data, and structures of Fe^{III} complexes are available on the Journal's website.

Conflicts of Interest

The authors declare no conflicts of interest.

Acknowledgements

This work was supported by the Australian Research Council (DP140100092) and the Australian Commonwealth Government (Australian Postgraduate Award to C. J. M. B).

References

- [1] R. Codd, *Coord. Chem. Rev.* **2008**, *252*, 1387. doi:10.1016/J.CCR.2007.08.001
- [2] C. J. Marmion, D. Griffith, K. B. Nolan, *Eur. J. Inorg. Chem.* **2004**, 3003. doi:10.1002/EJIC.200400221
- [3] A. Stintzi, K. N. Raymond, in *Molecular and Cellular Iron Transport* (Ed. D. M. Templeton) **2002**, pp. 273–319 (Marcel Dekker, Inc.: New York, NY).
- [4] A.-M. Albrecht-Gary, A. L. Crumbliss, in *Metal Ions in Biological Systems* (Ed. A. Sigel, H. Sigel) **1998**, pp. 239–327 (Marcel Dekker, Inc.: New York, NY).
- [5] A. Butler, *Nat. Struct. Biol.* **2003**, *10*, 240. doi:10.1038/NSB0403-240
- [6] R. C. Hider, X. Kong, *Nat. Prod. Rep.* **2010**, *27*, 637. doi:10.1039/B906679A
- [7] I. J. Schalk, M. Hannauer, A. Braud, *Environ. Microbiol.* **2011**, *13*, 2844. doi:10.1111/J.1462-2920.2011.02556.X
- [8] W. Neumann, M. Sassone-Corsi, M. Raffatellu, E. M. Nolan, *J. Am. Chem. Soc.* **2018**, *140*, 5193. doi:10.1021/JACS.8B01042
- [9] D. J. Raines, J. E. Clarke, E. V. Blagova, E. J. Dodson, K. S. Wilson, A.-K. Duhme-Klair, *Nat. Catal.* **2018**, *1*, 680. doi:10.1038/S41929-018-0124-3
- [10] E. W. Price, C. Orvig, *Chem. Soc. Rev.* **2014**, *43*, 260. doi:10.1039/C3CS60304K
- [11] P. J. Blower, *Dalton Trans.* **2015**, 4819. doi:10.1039/C4DT02846E
- [12] T. W. Price, J. Greenman, G. J. Stasiuk, *Dalton Trans.* **2016**, 15702. doi:10.1039/C5DT04706D
- [13] C. J. Adams, J. J. Wilson, E. Boros, *Mol. Pharm.* **2017**, *14*, 2831. doi:10.1021/ACS.MOLPHARMACEUT.7B00343
- [14] R. Codd, T. Richardson-Sanchez, T. J. Telfer, M. P. Gotsbacher, *ACS Chem. Biol.* **2018**, *13*, 11. doi:10.1021/ACSCHEMIBIO.7B00851
- [15] G. Fischer, U. Seibold, R. Schirmacher, B. Wängler, C. Wängler, *Molecules* **2013**, *18*, 6469. doi:10.3390/MOLECULES18066469
- [16] S. Heskamp, R. Raavé, O. C. Boerman, M. Rijpkema, V. Goncalves, F. Denat, *Bioconjug. Chem.* **2017**, *28*, 2211. doi:10.1021/ACS.BIOCONJCHEM.7B00325
- [17] J. R. Dilworth, S. I. Pasco, *Chem. Soc. Rev.* **2018**, *47*, 2554. doi:10.1039/C7CS00014F

- [18] N. B. Bhatt, D. N. Pandya, S. Rideout-Danner, H. D. Gage, F. C. Marini, T. J. Wadas, *Dalton Trans.* **2018**, 13214. doi:10.1039/C8DT01841C
- [19] J. P. Holland, Y. Sheh, J. S. Lewis, *Nucl. Med. Biol.* **2009**, *36*, 729. doi:10.1016/j.nucmedbio.2009.05.007
- [20] J. P. Holland, V. Divilov, N. H. Bander, P. M. Smith-Jones, S. M. Larson, J. S. Lewis, *J. Nucl. Med.* **2010**, *51*, 1293. doi:10.2967/JNUMED.110.076174
- [21] N. Pandit-Taskar, J. A. O'Donoghue, J. C. Durack, S. K. Lyashchenko, S. M. Cheal, V. Beylergil, R. A. Lefkowitz, J. A. Carrasquillo, D. F. Martinez, A. M. Fung, S. B. Solomon, M. Goenen, G. Heller, M. Loda, D. M. Nanus, S. T. Tagawa, J. L. Feldman, J. R. Osborne, J. S. Lewis, V. E. Reuter, W. A. Weber, N. H. Bander, H. I. Scher, S. M. Larson, M. J. Morris, *Clin. Cancer Res.* **2015**, *21*, 5277. doi:10.1158/1078-0432.CCR-15-0552
- [22] P. K. E. Börjesson, Y. W. S. Jauw, R. Boellaard, R. de Bree, E. F. I. Comans, J. C. Roos, J. A. Castelijns, M. J. W. D. Vosjan, J. A. Kummer, C. R. Leemans, A. A. Lammertsma, G. A. M. S. van Dongen, *Clin. Cancer Res.* **2006**, *12*, 2133. doi:10.1158/1078-0432.CCR-05-2137
- [23] E. C. Dijkers, T. H. Oude Munnink, J. G. Kosterink, A. H. Brouwers, P. J. Jager, J. R. de Jong, G. A. van Dongen, C. P. Schroeder, M. N. Lub-de Hooge, E. G. de Vries, *Clin. Pharmacol. Ther.* **2010**, *87*, 586. doi:10.1038/CLPT.2010.12
- [24] F. Guérard, Y.-S. Lee, R. Tripier, L. P. Szajek, J. R. Deschamps, M. W. Brechbiel, *Chem. Commun.* **2013**, 1002. doi:10.1039/C2CC37549D
- [25] J. P. Holland, N. Vasdev, *Dalton Trans.* **2014**, 9872. doi:10.1039/C4DT00733F
- [26] L. R. Perk, G. W. M. Visser, M. J. W. D. Vosjan, M. Stigter-van Walsum, B. M. Tjink, C. R. Leemans, G. A. M. S. van Dongen, *J. Nucl. Med.* **2005**, *46*, 1898.
- [27] M. Patra, A. Bauman, C. Mari, C. A. Fischer, O. Blacque, D. Haussinger, G. Gasser, T. L. Mindt, *Chem. Commun.* **2014**, 11523. doi:10.1039/C4CC05558F
- [28] W. Tieu, T. Lifa, A. Katsifis, R. Codd, *Inorg. Chem.* **2017**, *56*, 3719. doi:10.1021/ACS.INORGCHEM.7B00362
- [29] T. Richardson-Sanchez, W. Tieu, M. P. Gotsbacher, T. J. Telfer, R. Codd, *Org. Biomol. Chem.* **2017**, *15*, 5719. doi:10.1039/C7OB01079F
- [30] M. Briand, M. L. Aulsebrook, T. L. Mindt, G. Gasser, *Dalton Trans.* **2017**, 16387. doi:10.1039/C7DT03639F
- [31] S. E. Rudd, P. Roselt, C. Cullinane, R. J. Hicks, P. S. Donnelly, *Chem. Commun.* **2016**, 11889. doi:10.1039/C6CC05961A
- [32] C. J. M. Brown, M. P. Gotsbacher, J. P. Holland, R. Codd, *Inorg. Chem.* **2019**, *58*, 13591. doi:10.1021/ACS.INORGCHEM.9B00878
- [33] K. M. Ledyard, A. Butler, *J. Biol. Inorg. Chem.* **1997**, *2*, 93. doi:10.1007/S007750050110
- [34] Z. Hou, C. J. Sunderland, T. Nishio, K. N. Raymond, *J. Am. Chem. Soc.* **1996**, *118*, 5148. doi:10.1021/JA9600946
- [35] Z. Hou, K. N. Raymond, B. O'Sullivan, T. W. Esker, T. Nishio, *Inorg. Chem.* **1998**, *37*, 6630. doi:10.1021/IC9810182
- [36] R. Codd, C. Z. Soe, A. A. H. Pakchung, A. Sresutharsan, C. J. M. Brown, W. Tieu, *J. Biol. Inorg. Chem.* **2018**, *23*, 969. doi:10.1007/S00775-018-1585-1
- [37] G. Anderegg, F. L'Eplattenier, G. Schwarzenbach, *Helv. Chim. Acta* **1963**, *46*, 1400. doi:10.1002/HLCA.19630460435
- [38] A. Evers, R. D. Hancock, A. E. Martell, R. J. Motekaitis, *Inorg. Chem.* **1989**, *28*, 2189. doi:10.1021/IC00310A035
- [39] S. Dhungana, P. S. White, A. L. Crumbliss, *J. Biol. Inorg. Chem.* **2001**, *6*, 810. doi:10.1007/S007750100259
- [40] Y. Toporivska, E. Gumienna-Kontecka, *J. Inorg. Biochem.* **2019**, *198*, 110753
- [41] J. P. Holland, *Inorg. Chem.* **2020**, *59*, 2070.
- [42] R. K. Shervedani, Z. Akrami, F. Yaghoobi, M. Torabi, H. Sabzyan, *J. Phys. Chem. C* **2019**, *123*, 29932. doi:10.1021/ACS.JPCC.9B07407
- [43] T. J. Telfer, T. Richardson-Sanchez, M. P. Gotsbacher, K. P. Nolan, W. Tieu, R. Codd, *Biomaterials* **2019**, *32*, 395. doi:10.1007/S10534-019-00175-7
- [44] E. W. Price, B. M. Zeglis, J. F. Cawthray, J. S. Lewis, M. J. Adam, C. Orvig, *Inorg. Chem.* **2014**, *53*, 10412. doi:10.1021/IC501466Z